Available online at www.sciencedirect.com
SCIENCE DIRECT
Polymer 47 (2006) 1187–1196
polymer
www.elsevier.com/locate/polymer

Energy transfer in the photoluminescence of poly(3-thiophene acetic acid)–poly(vinyl alcohol) blends

Paulo N.M. dos Anjos [a], Ernesto C. Pereira [b,*], Yara G. Gobato [c,1]

[a] Departamento de Ciências Exatas e Tecnológicas, Universidade Estadual de Santa Cruz, CEP 45662-000 Ilhéus, BA, Brazil
[b] Laboratório Interdisciplinar de Eletroquímica e Cerâmica, Departamento de Química, Universidade Federal de São Carlos, São Carlos, SP, Brazil
[c] Laboratório de Semicondutores, Departamento de Física, Universidade Federal de São Carlos, CEP 13560-970 São Carlos, SP, Brazil

Received 27 June 2005; received in revised form 16 December 2005; accepted 19 December 2005

Abstract

We have investigated the optical properties of polymeric blend poly(3-thiophene acetic acid)–poly(vinyl alcohol). We have observed two band sets with different features in the photoluminescence spectrum. One set shows a band peak at 560 nm and the other shows two band peaks at 670 and 710 nm. We have analyzed the polarization and temperature dependence of photoluminescence spectrum. We have observed that the first set is unpolarized and shows weak temperature dependence, while the second one shows strong temperature dependence and a polarized band at 710 nm. These results were interpreted as evidence of energy transfer associated with migration and trapping of excitons in the poly(3-thiophene acetic acid) chains using a kinetic model with we estimated the energy of the trap site for the triplet exciton emissions.

Keywords: Luminescence; Energy transfer; Conducting polymers

1. Introduction

In the last two decades oligomer and polymer thiophene derivatives have been investigated due to their potential application in organic electronic devices [1], light emitting diodes [2,3], photodetectors [4] and solar cells [5]. In order to develop such applications and obtain suitable efficiency and durability, it is necessary to understand their photophysical and photochemical properties in solution, thin films and blends.

Photosensitive materials based on blended polymers have proved essential in developing of optical and electro-optical devices. Some of these materials were composed of polymers such as poly(acrylic acid, PAA) [6] and poly(methyl methacrylate, PMMA) [7]. These polymers had properties such as low cost, high processability, high light transparency and chemical and thermal stabilities. Another important polymer is the poly(vinyl alcohol, PVA), which is a commercial polymer, usually produced by acidic or basic hydrolysis of the poly(vinyl acetate, PVAC). Its properties depend on its molecular weight and degree of hydrolysis. Among its possible composite materials, because of the high quality of its films, it cam be useful as a support in many industrial applications, including non-linear optical devices [8].

Up to now, in electro-optical applications, most of the polymer devices are based on modified poly(phenylene vinylene)s or polythiophenes. The vast majority of these polymers are soluble in organic only. Introduction of water-soluble conjugated polymers could render the processing of these materials (if ever produced and used on the large scale) more friendly to the environment. In addition, an approach to make solid polymer solutions is based on the polymer blending. Polymer blends do often lead to phase separation. This is because of the low entropy of mixing of polymer chain. There are fewer ways of distributing the constituents and this causes microphase separated materials. To suppress the phase separation in the polymer blend, one must influence the other part of the free energy of mixing, which is the enthalpic part. Adding attractive interactions between the matrix and the polymer to be dissolved can be sufficient to make solid solutions with better molecular dispersions.

On the other side, the photophysics of thiophenes in solution is well understood, which is a good base for the interpretation of their properties in the solid state [9,10], in which new decay channels open up, due to intermolecular interactions, defects

* Corresponding author. Tel./fax: +55 16 3351 8214.
E-mail address: decp@power.ufscar.br (E.C. Pereira).
[1] Also from Departamento de Física, Universidade Federal de Santa Catarina, Santa Catarina, Brazil.

0032-3861/$ - see front matter © 2005 Elsevier Ltd. All rights reserved.
doi:10.1016/j.polymer.2005.12.078

and impurities. In addition, the molecular organization has a fundamental role, because it can affect both the nature and the decay mechanism of excited states. In particular, the periodic interactions between the molecules in ordered structures induce the formation of collective excited states (exciton) [11] with different properties compared to isolated molecules. Comparing these two different cases, isolated molecules in solution and the strongly interacting molecules in the solid state, the intermolecular and intramolecular interactions in these systems can be described. In principle, the same properties of an isolated single crystal are observed in a polycrystalline films. The main difference is that the latter contains a large number of trapping sites (e.g. dislocations, local aggregation and defects) at the grain boundaries that make difficult to distinguish the molecular properties from those of the disorder-induced states. In fact, delocalized excitons were not observed in polycrystalline films and blends due to the structural disorder. Therefore, it is more reasonable to assign an excited state to a localized site that presents a molecular character. Consequently, excited states in these systems can be compared to those observed in thiophene solutions. However, in contrast to single molecules, their decay dynamics are faster by several orders of magnitude and have non-exponential behavior [12–15]. Another effect that can be observed is the charge transfer excitation (CT), which occurs at certain sites, such as two-molecule clusters, where the molecules are in tail-to-tail or head-to-head configuration [16].

The intersystem crossing (ISC) can also explain the decay mechanism in these systems. It is important to stress that the ISC explanation is not completely equivalent to that of the trapping sites (described above) as the CT state can decay quickly due to recombination, but during its lifetime may also undergo intersystem crossing (ISC). In addition, due to the fast decay dynamics of the excited states in the solid state, it is rather unlikely that triplet states can be formed by the usual spin-flip molecular mechanism. However, singlet excited states may have other channels for triplet conversion. These include: (a) singlet excited state fission into triplet pairs, which requires an excitation energy that is at least twice the triplet energy; (b) the conversion by a localized excitation associated with the formation of an excimer. Thus, excited dimers or CT states can occur in the disordered solid-state [17,18].

In this paper, we have studied optical properties of poly(3-thiophene acetic acid)–poly(vinyl alcohol), PVA–PTAA, blends in solution and in the solid state. We have measured the photoluminescence spectra of these blends as function of temperature and laser intensity. We have also analyzed the polarization state of photoluminescence spectrum. Two different spectral emission profiles were observed and interpreted as an evidence of energy migration in the poly(3-thiophene acetic acid) chains.

2. Experimental part

The PTAA was prepared by the oxidative polymerization of 3-thiopheneacetic acid (Sigma Co.) with ferric chloride (Merck) in chloroform (Merck) under dry nitrogen purge flow as described elsewhere [19,20]. The poly(vinyl alcohol), PVA, (Mallinckrodt Chemical Co., MW 133,000 and 99% hydrolyzed) was used as received. The PTAA–Na salt solution was prepared by dissolving PTAA in ultra pure water (MilliQ) and adding diluted NaOH. The PTAA–PVA blends were prepared by dissolving 0.5 g of PVA in 15.0 ml MilliQ water under mild heating and stirring, after which 5.0 mg of PTAA–Na salt were and added to the solution to yield a transparent PVA–PTAA solution. The solution was homogenized, poured into a Petri plate and cooled to room temperature. The solvent spontaneously evaporated at room temperature and under atmospheric pressure to give a transparent, orange, plastic film (PVA–PTAA blend).

The absorption spectra were measured using an ultraviolet–visible–NIR Cary 5G Varian Spectrophotometer. The photoluminescence spectra were recorded using a 457.9 nm line Coherent Ar^+ Spectra Physics and Spex 500 M single monochromator coupled to a thermoelectrically cooled R5108 Hamamatsu photomultiplier. The laser spot had a 0.2 cm^2 area. The experiments were performed at different temperatures using a JANIS closed system He cryostat.

The photoluminescence spectra (PL) were recorded using two different setups as presented schematically in Fig. 1. In the front-face (FF) setup, the emission was measured positioning the detection system in front of the sample. In the second setup (denoted right-angle (RA)) the detection of the luminescence was performed at 90° to that used in the FF setup. To simplify, FF-PL denotes the emission spectra measured using the FF setup and RA-PL denotes the RA setup. In order to analyze the

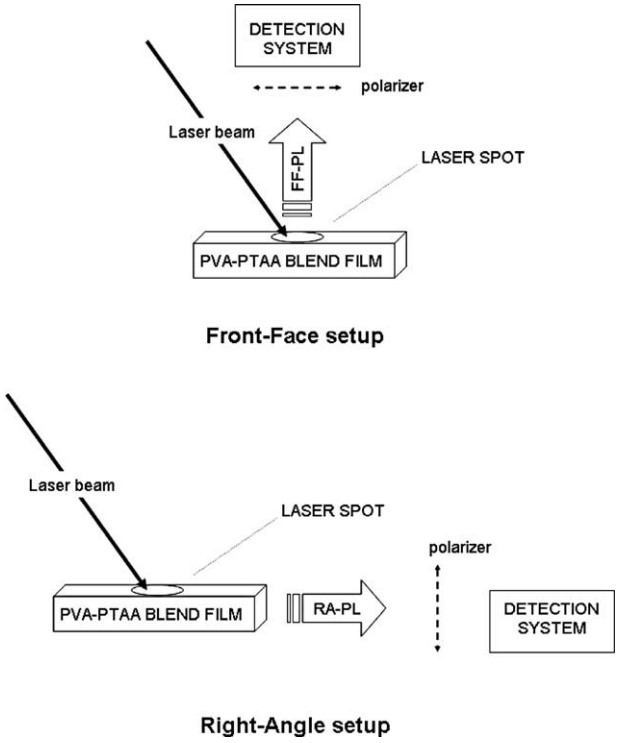

Fig. 1. Schematic diagram showing the front-face (FF, top) and right-angle (RA, bottom) setups for the detection of the luminescence emissions originating from the laser spot in the PVA–PTAA blend and from outside the laser spot.

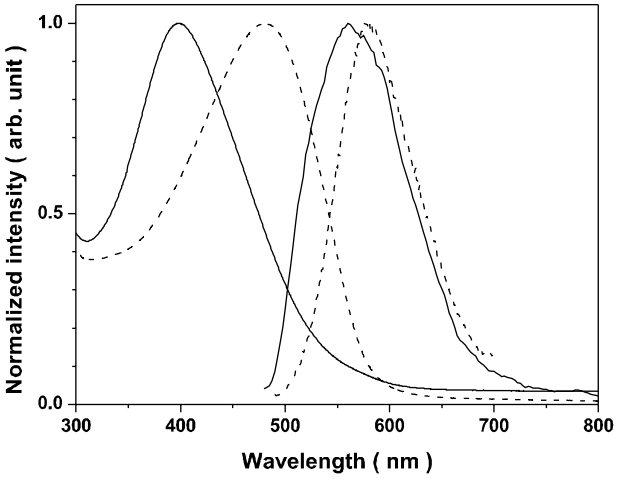

Fig. 2. Absorption and emission spectra for PTAA and PVA in aqueous solution (dashed line) and as a blend (solid line).

polarization of the emitted light for each setup, a polarizer was positioned at the entrance of the monochromator.

Calculations for geometry optimizations of the some 3-thiopheneacetic acid oligomers were made. On the basis of these geometries, we described the excited states hat promoted the photoluminescence in the PTAA–PVA blend. The geometries were optimized at the Hartree–Fock semi empirical Austin Model (AM1) [21] using the quantum chemistry package GAMESS [22]. For the geometry optimization of the oligothiophenes, the molecules were augmented from dimer to hexamer. That AM1 method had been reported to give ground-state geometries in good agreement with the results of X-rays diffraction studies [23,24].

3. Results

In Fig. 2 the absorption and emission spectra of the PVA and PTAA dissolved in aqueous solution and for the PVA–PTAA blend are shown. In solution (dashed line), the absorption and emission spectra are characteristic of isolated polythiophenes (PT) electronic transitions, which the spectrum profiles are associated with the distribution of the oscillator strength in regards to the conformational variation of the PT chains. Due to the low PTAA and PVA concentrations, the chains interact only weakly and the main influence on the spectral parameters (stokes shift and bandwidths) is the solvent effect. However, comparing the absorption and emission spectra for the PVA–PTAA blend with the spectra from solution, important changes can be observed. In the blend, the interaction between the PVA and PTAA chains is stronger than the PTAA–PTAA interaction in solution. That difference resulted in a different distribution of the oscillator strength as we compared the spectra in solution with the shifted the emission and absorption spectra in the blend film (solid line).

Table 1 shows the spectroscopic parameters of the absorption and emission of the PVA–PTAA systems in solution and in the blend. Comparing the data one can be noted that the peaks for both emission and absorption spectra in the blend are blue shifted in regards to those of the solution.

As one can be seen in Fig. 3, the luminescence spectra of the FF-PL and RA-PL for the PVA–PTAA blend are different. That difference came out because the luminescence of the PTAA–PVA blend exhibits a singular feature, two distinct emissions. One of them is observed coming out directly from the laser spot with a yellow hue, that we measured collecting the light using the front-face setup. The second emission was observed spreading outside the laser spot area, but could not be detected into the laser spot, this had occurred mainly due to the higher intensity of the yellow emission. That emission outside the laser spot had a reddish hue and because it spread in the blend film was detected more conveniently using the RA setup. It is interesting note that in the FF-PL the low energy tail in the emission spectrum should be related to those two reddish emissions, but they had much lower intensities, because that could not be distinguished.

The FF-PL (dotted line) showed only one broad asymmetric band with maximum intensity at 560 nm (2.21 eV) and a bandwidth of 114 nm (0.43 eV). This emission was attributed to a radiative decay of a localized-singlet exciton, which was generated by direct absorption at sites on the thiophene backbone [25–28]. The RA-PL (continuous line) presented three emission bands. The lower intensity band at 560 nm is due to the scattered luminescence coming out from the laser spot. The other two bands having maximum intensities at

Table 1
Spectroscopic parameters for the absorption and emission bands of the PVAPTAA systems in solution and in the blend

	Absorption		Emission		Stokes shift,[a] eV (nm)
	Peak energy, eV (nm)	Bandwidth,[b] eV (nm)	Peak energy, eV (nm)	Bandwidth, eV (nm)	
Solution	2.58 (481)	0.96 (161)	2.15 (576)	0.31 (91)	0.43 (95)
Blend	3.11 (398)	1.11 (142)	2.21 (560)	0.43 (114)	0.90 (162)
Energy shift[c]	0.53 (−83)		0.06 (−16)		
Blue/red shift	Blue shift		Blue shift		
Bandwidth variation[d]		0.15 (−19)		0.12 (−23)	
Variation %[e]		15%		39%	

Energies values in electron-volts and in round brackets the equivalent wavelength.
[a] Stokes shift calculated by subtracting the absorption peak from the emission peak.
[b] Bandwidth at half maximum.
[c] Band shift calculated by subtracting the solution peak from the blend peak.
[d] Bandwidth variation calculated by subtracting the solution peak from the blend peak.
[e] Variation % stands for relative bandwidth variation.

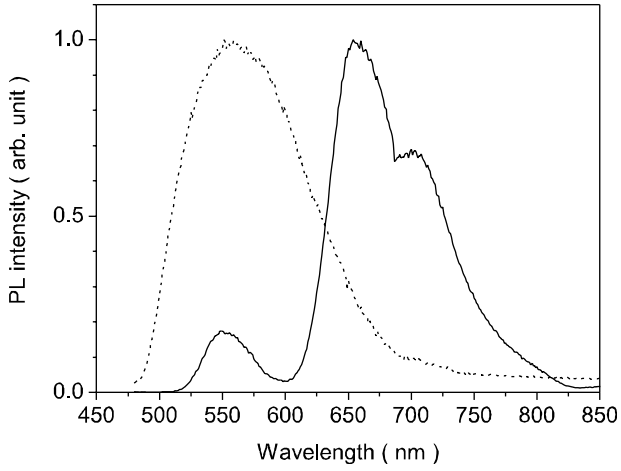

Fig. 3. PL spectra of the PVA–PTAA blend recorded using the FF (dashed line) and in the RA (solid line) detection setups.

670 nm (1.85 eV) and 710 nm (1.75 eV), respectively, were due to the emission spreading outside the laser spot. However, as discussed in the following section, these two emission bands cannot be related to the same process as that at the 560 nm.

Fig. 4 shows the polarization analysis for both PL spectra. The intensity of the FF-PL did not change as the orientation of the polarizer was varied from a parallel (0°) to a perpendicular position (90°) with respect to the laser excitation (Fig. 4 (A)). On the other hand, the RA-PL exhibited a polarized band (Fig. 4(B) (solid line)). When the axis of the polarizer was perpendicular to the excitation polarization, the band peaked at 700 nm had its intensity reduced and it was covered by the emission at 650 nm (dotted line), which remained with the same intensity as polarizer was parallel, indicating no polarization. When the polarizer was set parallel, both bands could be observed again. One possible cause for this polarization could be a wave guiding effect, as observed in materials that are coated by another material with lower refraction index. Normally, these modes of propagations are dependent on parameters such as the refraction indexes of materials, the optical path, the incidence angle of the light beam, the thickness of the material and its shape. In the PTAA–PVA blend, we found that those parameters had no influence on the polarized emission spectra. Samples with different thickness, optical path and shapes had same spectra and they were unaffected by the incidence angle of the laser beam. Because that, wave guiding was discarded as the mechanism for the polarization. These two bands, one polarized and the other not polarized, indicating that some PTAA chains were aggregated in regions of oriented crystalline PVA, while other chains were segregated into the non-oriented amorphous PVA, even though the PVA is not crystalline polymer, in solid films is commonly observed some regions with some degree of crystallinity. In other work with polythiophene blended with polyethylene [29] had been showed that the occurred an alignment of the polythiophene aggregates to with to the polyethylene chain, while the isolate chains are randomly distributed in the blend. In the case of the PTAA–PVA blend is

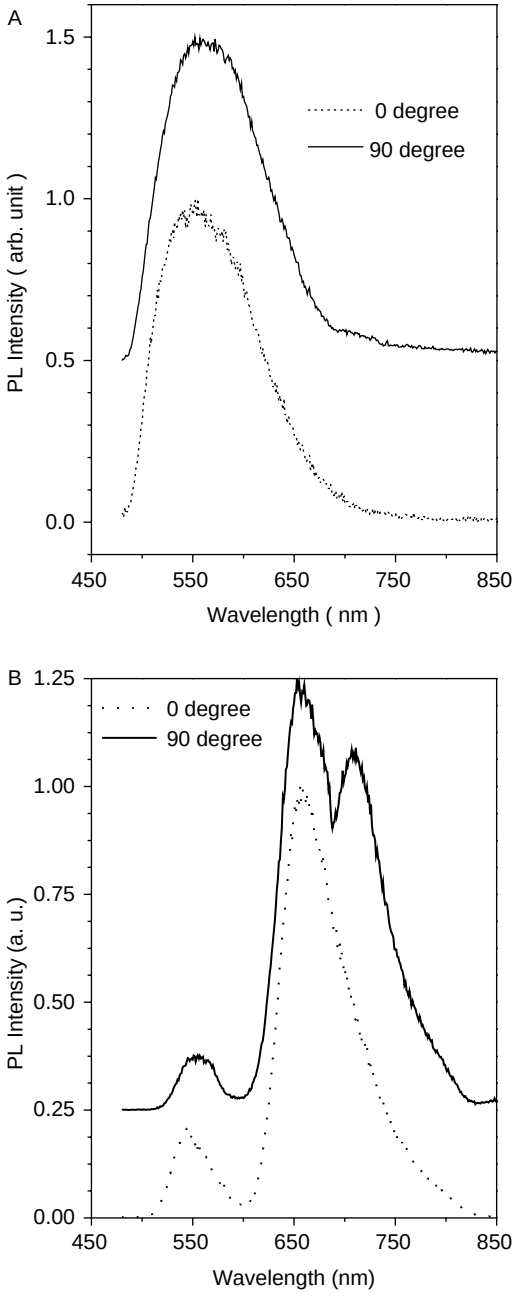

Fig. 4. PL spectra of the PVA–PTAA blend when the polarizer position was parallel (solid line) and perpendicular (dashed line) to the polarization plane of the laser beam; (A) is for FF detection setup and (B) RA detection setup. The spectra have been off-set slightly for ease of comparison.

expected that a similar effect occurs because the PVA is a semicrystaline polymer that, usually, have some high crystalline degree even without drawing. The polarization of the band at 710 nm is related to some sites in the PTAA backbone that have a specific orientation in relation to chain orientation.

The RA-PL was also analyzed as function of the laser intensity. As shown in Fig. 5(A), the laser intensity was increased eight-fold and the intensity of the spectra increased linearly (Fig. 5(B)). In addition, the band shapes did not change indicating that the luminescence process was a linear optical phenomenon, which ruled out processes such as multiphoton

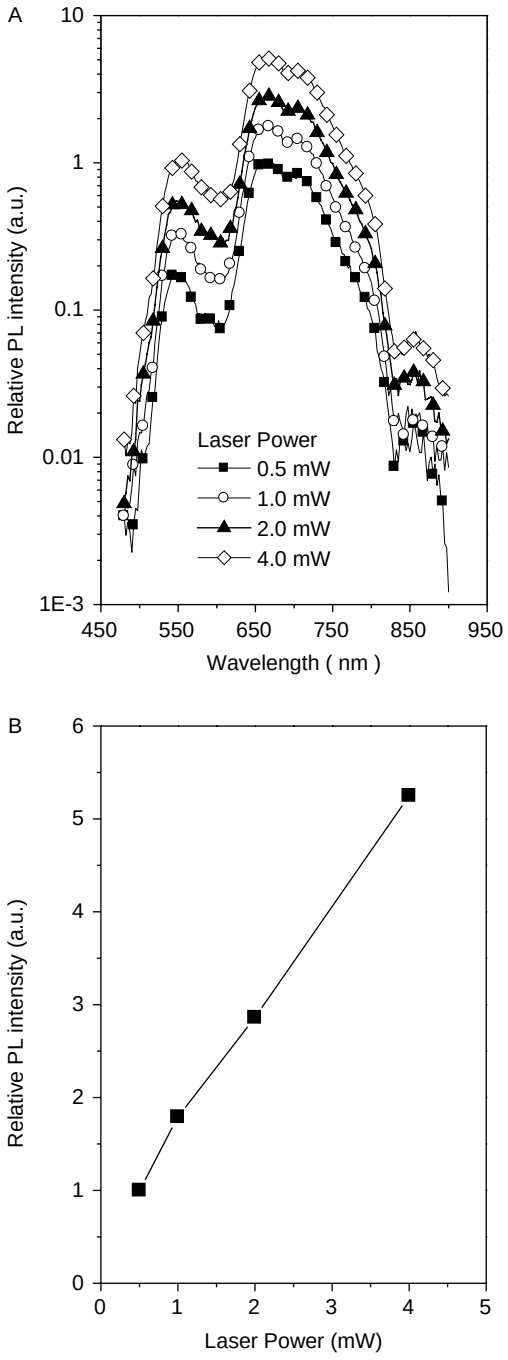

Fig. 5. (A) PL intensity for the RA setup as a function of the excitation power. (B) Relative PL intensity vs. laser power at 660 nm. The spectra have been offset slightly for ease of comparison.

absorption, refractive index variation and exciton annihilation in the explanation the data obtained.

The emission intensity profile for the band in the 500–600 nm (2.5–2.1 eV) range had a slight decrease as the temperature increased from $T=20$ to 160 K. On other hand, for the bands in the 600–850 nm (2.1–1.5 eV) range, the relative PL intensity profiles strongly decreased with increasing temperature in the same values. This temperature effect was clearly visible when comparing the relative intensities of the band peaks, as shown in Fig. 6(C). For the band at 500–600 nm (open circle) there was a very weak tendency to decrease (approx. 10%), while a stronger tendency (approx. 55%) was observed for the bands at 600–850 nm (solid circle). The behavior of the relative PL intensities with the temperature can be related to different mechanisms for each energy process in the radiative decay that is assigned to the emission bands. This will be discussed in the following section.

4. Discussion

Photoluminescence in conjugated polymers is due to excitonic emission, but the exact nature and kinetics of excitons in such systems remains under investigation. In some studies, it has been suggested that those photo-excitations are free carriers as the Coulombic interaction of an electron–hole pair within the exciton is negligible [30,31]. Other studies suggest that the excitons are localized in the polymer chain, i.e. similar to Frenkel excitons [32,33].

From a different point of view, most films and blends of conjugated polymers are disordered systems and, as such, the results of optical experiments should be interpreted considering a molecular model, where the polymer is treated as an ensemble of sites that are subjected to both energetic and positional disorder [34–36].

Photo-excitation generates excitons localized at some sites. Thus, such excitons can migrate towards lower energy sites, undergoing radiative recombination or non-radiative decay. In fact, the observed Stokes shift can, at least in many cases, be attributed to an incoherent migration of excitons before recombination [37–41].

The diffusion of the excited states may include both 3D diffusion on and between chains, as well as 1D diffusion of exciton along the chain. The diffusion process allows the exciton to probe many sites during its lifetime, higher lifetime more spreading of the energy. Because singlet excitons had very short lifetime, the diffusion process for they is more limited to short range, confining the exciton to 1D diffusion and reducing the possibilities for 3D diffusion. This confinement of singlet excitons should be responsible for the emission band at 560 nm, which was observed only inside the laser spot and not spreading outside to blend film.

The spectroscopic parameters obtained from the absorption and emission spectra (Fig. 2 and Table 1) indicate that the interaction between PTAA and PVA chains in the blend are different from those observed in the aqueous dissolved material. The onsets of absorption spectra were the same in the solution and in the solid phase. On the other hand, the absorption peak for the blend was blue shifted and this indicated a different PTAA organization in the blend [42–44]. In this case, the 0–0 transitions are very weak and this decreased the derivative of the low energy side in the absorption curve. As expected, there is a decrease in the half-height bandwidth (an increase in the energy distribution) comparing the solution and blend film. Moreover, there was almost no difference in the emission spectra. For films of poly(alkyl thiophenes), Gierschner et al. [45] attributed the Stokes shift to the formation of aggregates in the polymer

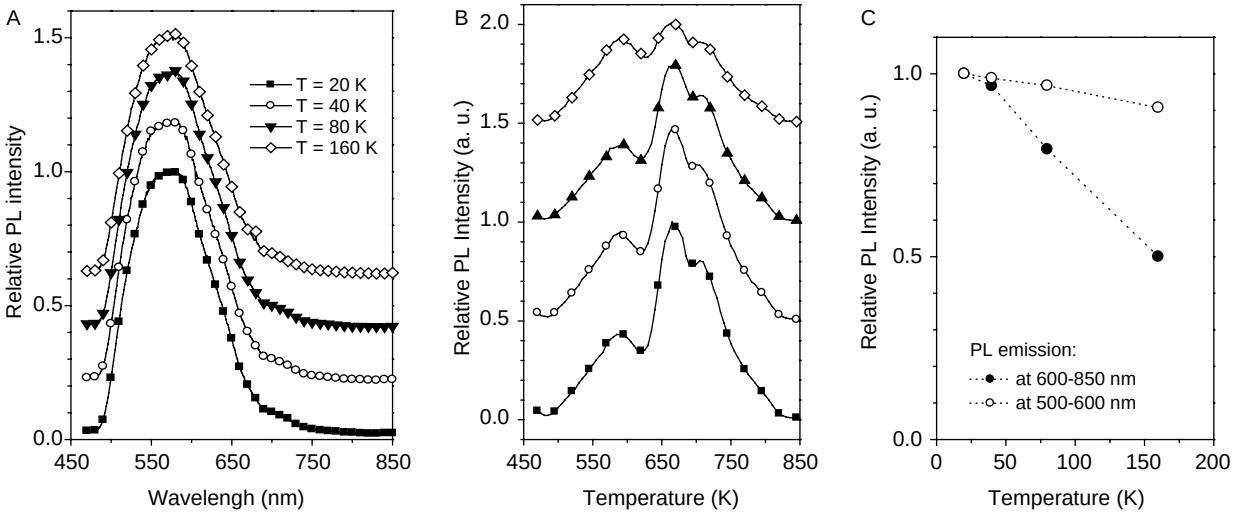

Fig. 6. PL intensity as a function of the temperature for the FF (A) and the RA (B) setups. (C) Relative PL intensity vs. temperature at 560–600 nm range (open dot) and relative PL intensity vs. temperature at 600–850 nm (solid dot). The spectra have been off-set slightly for ease of comparison.

blends. In the results presented here, for the PVA–PTAA blends, the Stokes shift observed of 0.90 eV could be related to aggregation, to differences in the interaction between the PTAA chains and the solution or even to changes in the conformational motion of the chains in solution. All of these possibilities are related to changes in the fundamental state of the material.

Although the mechanism of the differences between the solubilized blends and films is not clear, the observed changes in the behavior for the films were in agreement with a molecular exciton model used to describe energy diffusion [28–30].

In solution, the photoluminescence (PL) has only one broad band, with a peak at 576 nm. However, in the blend the photophysics follow other radiative paths, as indicated by the two different spectra obtained in the FF and RA detection setups. The PVA–PTAA blend presents two different radiative mechanisms operating simultaneously. One is similar to that which exists in solution and the other appears when the PVA and PTAA are in the solid phase. This is observed as an emission band in the red range of the spectrum (650–850 nm), as shown in Fig. 3.

These bands were attributed to triplet excitons because the energies values had been correlated with other theoretical and experimental results reported in literature [46–51], which showed that the dependence of the triplet energy with the number of monomers is much weak. Such difference is only lowered by about 0.2 eV when going from the dimers to the hexamers of thiophenes. The stronger confinement of the triplet excitons in oligothiophenes (in regards to the singlet excitons) was confirmed in other experimental works, such as: optical detected magnetic resonance (ODMR) measurements, showing a weak chain-length dependence of the spin–spin separation parameter [52]. The energies observed in ours results were very similar to values measured for the triple energies with respect to the ground state in oligo [50] and polythiophenes [51]. The band at 670 nm (1.85 eV) was assigned to a triplet exciton, T_n, delocalized in a segment of the chain with several units (between, while the band at 700 nm (1.75 eV) was attributed to a triplet exciton, T_1, localized in a smaller segment (dimer or trimer), which it should be the first triplet state. In fact, higher energy triplet state must not be as localized as the lower energy triplet exciton (the smaller confinement of the wave function in the triple state can be rationalized by the fact that it lie at higher energy than the lower state and, hence, has a smaller binding energy). In addition, in order to corroborate those attributions we made a computation simulation of the polythiophene chain using the geometry optimization of some oligomers of PTAA. As can be note in the Diagram 1, the backbone of the PTAA chain for a hexamer is shown without the hydrogen and side groups to better view of the geometric features. In this case one can be observed that some small segment (indicated out by the rings with S_3 and S_4 into backbone) was positioned in a plan almost perpendicular to the adjacent rings in the chain. If we assume that geometry can be representative of some extension of the PTAA chain, that small segment can be one trapping site for the localized triplet exciton T_1 emitting with 1.77 eV energy, once that also should have a specific polarization for the emission as was observed in the polarization analysis of the emission. On the other side, the higher energy triplet T_n lost this polarization because it was not localized in such site, but spreaded over longer segment in the PTTA chain, so had a less specific geometry for emission.

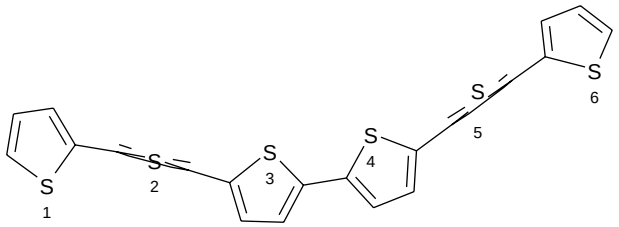

Diagram 1. Schematic representation of the optimized geometry of a hexamer without the hydrogen and side groups to better view of the plans of rings. Rings marked 3 and 4 are in the plane of the paper.

Luminescence from polymers containing conjugated chromophores has been investigated in solution and in solid state for many years [53–55] and some other systems have also been studied as polymer blends, such as polystyrene and polymethylmethacrilate [56]. Polystyrene is used as a matrix in styrene–phenylacetylene copolymers, locking the copolymer into a conformation that yields two principal emitting states. These two states correspond to a short and a long sequence of conjugated double bonds, each characterized by a distinct emission band. Using time-resolved fluorescence spectra it was shown that the energy transfer occurs in the short to long sequence of conjugated chromophores. Use of polymethylmethacrilate as a matrix was observed that emissions from the short sequence of conjugated chromophores are enhanced [57].

In the PVA–PTAA blend, polarized spectroscopy was used to investigate the characteristics of the two emission processes (Fig. 4). Specifically, when the polarization features of the emissions were analyzed, it was found that the intensity of the FF-PL features was not polarization dependent. On the other hand, RA-PL exhibited polarization dependence.

In the PVA–PTAA system, the two emission processes present different temperature dependencies and this can be related to different trap energy levels. As observed in the low temperature range (Fig. 6(B)), the intensity for the band at 500–600 nm is not significantly changed, while the emission bands in the 650–800 nm range decrease as the temperature is increased. To explain this difference a schematic model for the energy migration and trapping mechanisms can be considered. The trapping mechanism may be static or dynamic, depending on the geometric requirements for the formation of the trap. If the energy of the trapping site is lower than that of the exciton, without geometric rearrangement, then it is a static trap and the trapping rate may not depend on temperature at low values. But, if a significant geometric rearrangement is required for trapping to occur, the rate of trapping may be temperature dependent. Thus, dynamic trapping is thermally assisted. The trapping is typically inversely dependent on temperature since thermal energy enhances detrapping. However, the static and dynamic mechanisms can have different temperature dependences. This is illustrated by the simple kinetic scheme shown in Fig. 7.

We can obtain an equation to describe the temperature dependence of the triplet emission if we consider a mobile singlet exciton in the state, X_m, and a trapping site concentration, T_t. It is assumed that the activation energies ΔE_t^* and ΔE_d^* are required for the trapping and detrapping processes, respectively. Also, in the absence of other annihilation processes, the rate equations X_m and T_t are:

$$\frac{dX_m}{dt} = -(\Gamma_m + K_t)X_m + I_{ex} \quad (1)$$

$$\frac{dT_t}{dt} = -(\Gamma_t + K_d)T_t + K_t X_m \quad (2)$$

In Eqs. (1) and (2), Γ_m and Γ_t are pseudo-first order constant rate for producing X_m and for its trapping, while I_{ex} is the rate of production of T_m by the laser excitation source. It is assumed

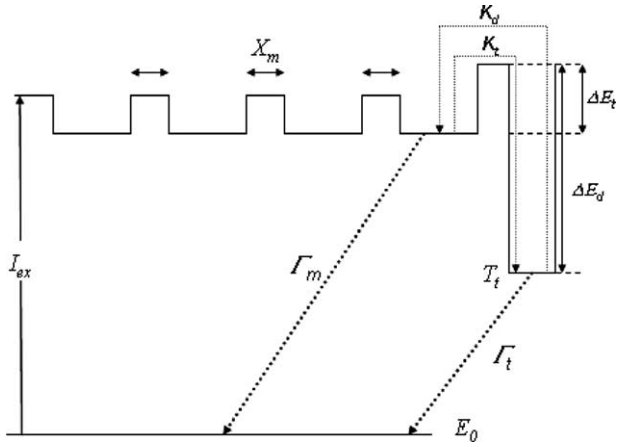

Fig. 7. Schematic representation of an illustrative kinetic scheme for static and dynamic trapping mechanisms acting in the energy migration.

that the T_t state is produced only by trapping the X_m exciton. Because of the high energy difference between ground and the excited states they are assumed to have no dependence on temperature. On the other side, the trapping and detrapping rate constants, K_t and K_d, respectively, can be dependent on temperature because the triplet energy difference between sites is low (0.2 eV) and only weakly dependent on chain size. In other words, the singlet exciton diffusion is more restrict and once it was trapped, it cannot be detrapped so easily and decay radiatively. The trapping and detrapping rate constants, K_t, and, K_d, are assumed to be an Arrhenius kinetic rate equation type:

$$K_t = A_t \exp\left(-\frac{\Delta E_t}{k_B T}\right) \quad (3)$$

$$K_d = A_d \exp\left(-\frac{\Delta E_d}{k_B T}\right) \quad (4)$$

where A_t and A_d are pre-exponential factors related to the trapping and detrapping probabilities for those processes, k_B is the Boltzmann constant and T the absolute temperature. If we assume that the T_t state is produced only by trapping the X_m, under steady-state conditions, the solutions for Eqs. (1) and (2) are:

$$X_m^{SS} = \frac{I_{ex}}{(\Gamma_m + K_t)} = I_{ex}(\Gamma_m + K_t)^{-1} = I_{ex}\left(1 + \frac{\Gamma_m}{K_t}\right)^{-1} \quad (5)$$

$$T_t^{SS} = \frac{\Gamma_t X_m^{SS}}{\Gamma_t + K_d} = X_m^{SS}\left(1 + \frac{K_d}{\Gamma_t}\right)^{-1} = I_{ex}\left(1 + \frac{\Gamma_m}{K_t}\right)^{-1}\left(1 + \frac{K_d}{\Gamma_t}\right)^{-1} \quad (6)$$

Eq. (6) represents the steady-state concentration for the triplet exciton in the trapping site and must be proportional to the luminescence. We can obtain a more simple approximate expression using the corresponding Taylor series expansion for the reciprocal terms in Eq. (6):

$$(1 + x)^{-1} = 1 - x + x^2 \ldots \quad (7)$$

We have, ruling out terms of second and high order, simplified the Eq. (6) to:

$$T_t^{SS} \cong I_{ex}\left(1-\frac{\Gamma_m}{K_t}\right)\left(1-\frac{K_d}{\Gamma_t}\right) \tag{8}$$

Simplifying the Eq. (8) once more by considering only the constant ratios as important factors, we obtain finally:

$$T_t^{SS} \cong I_{ex}\frac{\Gamma_m}{\Gamma_t}\frac{K_d}{K_t} \tag{9}$$

Substituting Eqs. (3) and (4) in Eq. (9) and rearranging the constant and exponentials the equation for T_t^{SS} is given by

$$T_t^{SS} \cong I_{ex}\frac{\Gamma_m}{\Gamma_t}\frac{K_d}{K_t} = I_{ex}\frac{\Gamma_m A_d}{\Gamma_t A_t}\exp\left(\frac{-\Delta E_d^*}{k_B T}\right)\exp\left(\frac{\Delta E_t^*}{k_B T}\right)$$

$$= I_{ex}\frac{\Gamma_m A_d}{\Gamma_t A_t}\exp\left(\frac{-\left(\Delta E_d^* - \Delta E_t^*\right)}{k_B T}\right) \tag{10}$$

In Eq. (10) the term $(\Delta E_d^* - \Delta E_t^*)$ represents the difference between the activation energies ΔE_t^* and ΔE_d^* that are required for the trapping and detrapping processes, it is, in fact, an effective deep of the trap for the excitons in term of energy offset. We denoted it as ΔE_t^{off}, so Eq. (10) became:

$$T_t^{SS}(T) = I_{ex}\frac{\Gamma_m A_d}{\Gamma_t A_t}\exp\left(\frac{-\left(\Delta E_t^{off}\right)}{k_B T}\right) \tag{11}$$

In Eq. (11), we explicated the temperature dependence of the $T_t^{SS}(T)$, because we want use it to analyze our data of spectral dependence on temperature. We consider a temperature of reference, T_0, such as, for example, $T_0 = 20$ K. Then, we compare $T_t^{SS}(T_0)$ with $T_t^{SS}(T)$ in other temperature, T_1. Making the ratio of $T_t^{SS}(T)$ in these two temperatures we can obtain after some algebra the following expression:

$$\ln\left(\frac{T_t^{SS}(T_1)}{T_t^{SS}(T_0)}\right) = \frac{\Delta E_t^{off}}{k_B}\left(\frac{1}{T_0}-\frac{1}{T_1}\right) \tag{12}$$

The Eq. (12) is quite important because with it we can estimate the ΔE_t^{eff} using the relative PL intensity measured in different temperature plotted in regards to difference between the respective reciprocal temperature. As can be seen in the Fig. 8, the plots show the results of linear fitting for the PL temperature dependence in the 600–850 nm range shown in Fig. 6.

From those data we obtained for the bands at 670 and 710 nm the trap energy offsets were 1.03 and 1.07 meV, respectively. Also, using same model to the band at 560 nm, the offset found was 0.16 meV. These figures are very significantly to understand why the one type of emission was more dependent on temperature than other. As can be note, the energy offset the 560 nm emission were almost six times lower than the offset for the other emissions a 670 and 710 nm. Comparatively, the exciton in 560 nm was a shallow trap even at low temperature, and the mechanism for trapping and detrapping are both effectives in such way that exciton concentration on steady state condition are not dependent on temperature. On the other hand, for the triplet excitons, they

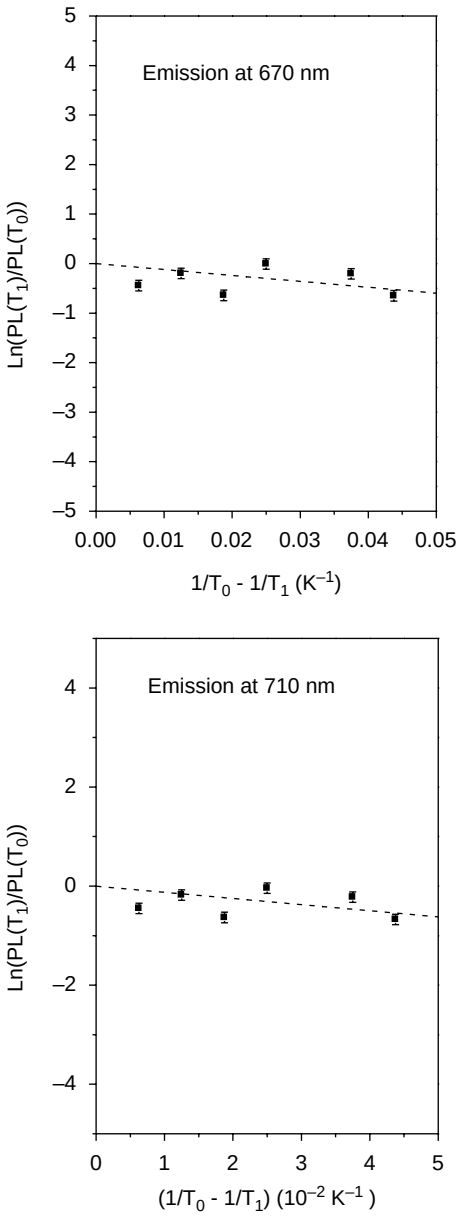

Fig. 8. Temperature dependence of relative photoluminescence intensity.

have higher offset, so only from some relatively higher temperature the detrapping process becomes more effective at higher temperature. In this case, T_t^{SS} decreases at high temperatures. Thus, the steady-state concentration exhibits inverted behavior when plotted against T, as can be observed in the Fig. 6 for the bands in the 600–850 nm range. However, the same behavior was not observed for the band in the 500–600 nm range. If it is assumed that, $\Delta E_t^{off} \approx 0$, for this process at low temperatures, then the quantum efficiency, $\phi_t(T)$, is independent of temperature which explains the results associated with this emission. In that case, the emission can be related to an intrachain process, while for the other emissions it is an interchain one.

Using the model proposed above, the data can be interpreted considering the steps: after absorption, fast thermalization brings the population down to the lowest singlet excited state,

S_1. This process is accompanied by a nuclear adjustment, which leads to a more planar geometry. The increased conjugation length of the planar structure is associated with a longer conjugation length. From that point, the excited state has two radiative pathways: one is direct radiative decay associated with singlet exciton trapping for the band in the 500–600 nm range and occurring in the laser spot where the energy density is quite high. The other process, which is related to the emission observed in the 600–850 nm range, is excitation diffusion between identical sites. In this process, the energy of excitation is not bound to the original absorbing chromophore but it is able to migrate by a series of interactions. Thus, the excitation is spread over a number of chromophores and moves through the blend structure. This energy migration can be observed as another component in the luminescence spectrum when a trapping mechanism leads to a radiative decay. As the lifetime for a singlet excited state is much lower than for long life states, energy migration is normally more effective for the latter species. This is due to the energy migration process, which is best visualized as a random walk. Thus, the energy migration occurs until a shallow trap promotes the deactivation of the long life states in a radiative pathway. The shallow trap is formed due to the difference in the energy between the long life sites that can occur from differences in conformational changes, impurities or end chain sites. The above model explains qualitatively many features of the experimental results. Although it is a good approximation for the PTAA–PVA system, more detailed investigation must be carry out to apply it to another system were other radiative and non-radiative processes were effective.

The nature of the emitter in the PTAA–PVA system cannot be attributed to the excited complex states, such as excimer or exciplex, because we not observed the main distinct signature for these species: the inverse relation between the monomer and complex PL intensity, the monomer emission decreases at high concentration while the complex state emission proportionally increases. The intensity of both emissions at 560 nm and in the 600–850 nm increase as the concentration of the PTAA. Furthermore, excimer formation requires strict geometric conditions to approach a sandwich-like orientation for the conjugate or aromatic units in the polymer chain. The acetic acid side group is a very steric one, which difficult such orientation for nearby thiophene units either intra- or intermolecular, also the low concentration of PTAA in PVA prevents high density for thiophene units. Another important feature of the side group is the possibility of forming hydrogen bonding with the hydroxyl group in the PVA or the formation of the ester bonding. The latter case is important because the blend becomes an interpenetrating network (IPN), which promotes rigid structural arrangement for the polymer components. Moreover, the evidence for the a triplet state emitter in this case of the PTAA–PVA blend film is the early evidence for enhancement of intersystem crossing (ISC) just observed in another PVA film doped with some molecular alkaloid as reported by de Souza and dos Anjos working with poly acrylic acid and PVA [58]. In that work it was observed an enhancement of triplet radiative rate at room temperature after the IPN was excitation in the singlet state. In the PTAA–PVA case, we can relate a similar picture because the excitation of the singlet state promotes a high density in the laser spot area, which can undergo the ISC process. The triplet exciton formed, then diffuses to outside the laser spot and approach the emitting site. In the case of this triplet energy migration, the donor and acceptor are chemically equivalent, but for one reason not all molecules in the backbone are equivalent (the geometry of the segments are oriented perpendicular to other) in such way that the triplet energy is slightly depressed at some point (as we had obtained with offset energy for the 650 and 710 nm bands), then the shallow trap is produced.

5. Conclusions

The PVA–PTAA blend exhibited two different luminescence spectra whose features depend on the position at which the light emitted is detected. When the direction is parallel to the excitation, the emission spectrum has only one broad peak at 560 nm (FF-PL). However, when the direction is perpendicular to the excitation, the PL spectrum (RA-PL) presents two broad bands that peak at 650 and 700 nm, respectively. Polarized spectroscopy demonstrates that FF-PL and RA-PL spectra have different polarization features. For FF-PL, the band has no polarization characteristics (isotropic emission). However, for the RA-PL emission the two bands have different polarization features. The band at 650 nm was isotropic, while the band at 700 nm was anisotropic. Such differences in the emission polarization are attributed to an energy migration process that promotes the RA-PL emission. Temperature dependence experiments in the low temperature interval (20–160 K) were interpreted with a kinetic model for static and dynamic trapping that shows that the FF-PL intensity is not altered with increasing temperature because the energy offset was too small ($\sim$0.16 meV), while the RA-PL intensity strongly decreased with higher temperature due to more deeper trapping with 1.03 and 1.07 meV for emission at 670 and 710 nm, respectively. These different dependencies were interpreted in terms of two different energy trapping processes that occur in the PVA–PTAA blend. The RA-PL process occurs by thermal assisted trapping (dynamic trapping). On the other hand, the FF-PL trapping process occurs without thermal assistance (static trapping). The energy trapping model proposed to explain the temperature dependence of each emission was quite simple, but represents an good approximation which can account for other systems to obtain he offset energy for trap sites. We considered two rate equations for the trapping process and Arrhenius temperature dependence for the trapping and detrapping rate constants, but a more elaborated model could be made if other processes must be incorporated.

Acknowledgements

The authors are grateful to FAPESP and CNPq for financial support.

References

[1] Garnier F. Acc Chem Res 1999;32:209.
[2] Segura JL. Acta Polym 1998;49:319.
[3] Heeger AJ. Solid State Commun 1998;107(11):673.
[4] Aihara S, Hirano Y, Tajima T, Tanioka K, Abe M, Saito N, et al. Appl Phys Lett 2003;82:511.
[5] Wöhrle D, Meissner D. Adv Mater 1991;3:129.
[6] Lessard RA, Manivannan SS. J Imaging Sci Technol 1997;41:228.
[7] Manivannan SS, Lessard RA. Thin Solid Films 1994;253:228.
[8] Manivannan G, Gangkakoti R, Lessard RA, Maillo G, Bolte M. J Phys Chem 1993;97:7228.
[9] Charra F, Fichou D, Nunzi J-M, Pfeffer N. Chem Phys Lett 1992;192:566.
[10] Chosrovian H, Grebner D, Rentsch S, Naarmann H. Synth Met 1992;52: 213.
[11] Klein G. Chem Phys Lett 2000;320:65.
[12] Wong KS, Bradley DDC, Hayes W, Ryan JF, Friend RH, Lindenberger H. J Phys C 1987;20:L187.
[13] Furukawa M, Mizuno KI, Matsui A, Rughooputh SDDV, Walker WC, et al. J Phys Jpn 1989;58:2976.
[14] Rothberg L, Hsu JP, Yan M, Wilson WL, Jedju TM, Hsieh BR. Proc SPIE Int Soc Opt Eng 1993;1910:122.
[15] Lemmer U, Mahrt RF, Wada Y, Greiner A, Bassler H, Gobel ED. Appl Phys Lett 1993;62:2827.
[16] Lanzani G, Frolov SV, Lane PA, Vardeny ZV, Nisoli M, De Silvestri S. Phys Rev Lett 1997;79:3066.
[17] Lanzani G, Cerullo G, Stagira S, De Silvestri S, Garnier F. Phys Rev B 1998);58:7740.
[18] Marks RN, Muccini M, Lunedi E, Michel RH, Murgia M, Zamboni R, et al. Chem Phys Lett 1998;227:49.
[19] Royappa AT, Rubner MF. Langmir 1992;8:3177.
[20] de Souza JM, dos Anjos PNM, Pereira EC, Gobato YG, dos Santos LS. Synth Met 2002;130:121.
[21] Dewar MJS, Zoebisch EG, Hearly EF, Stewart JJP. J Am Chem Soc 1985; 107:3902.
[22] Schmidt MW, Baldridge KK, Boatz JA, Elbert ST, Gordon MS, Jensen JH, et al. J Comput Chem 1993;14:1347.
[23] Bouwstra JA, Schouten A, Kroon J. Acta Crystalogr Sect B 1975;40:428.
[24] Hotta S, Waragai K. J Mater Chem 1991;1:835.
[25] Kenemitsu Y, Suzuki K, Masumoto Y, Tomiuchi Y, Shiraishi Y, Koruda M. Phys Rev B 1994;50:2301.
[26] Lanzani G, Nisoli M, De Silvestri S, Tubino R, Barbarella G, Zambianchi M. Phys Rev B 1995;51:13770.
[27] Lanzani G, Nisoli M, De Silvestri S, Tubino R. Chem Phys Lett 1996;251: 339.
[28] Wong KS, Wang H, Lanzani G. Chem Phys Lett 1998;288:59.
[29] Luzzati S, Elmino P, Bolognesi A. Synth Met 1996;76:23.
[30] Pakbaz K, Lee CH, Heeger AJ, Hagler TW, McBranch D. Synth Met 1994;64:295.
[31] Heeger AJ, Kivelson S, Schrieffer JR, Su WP. Rev Mod Phys 1988;60: 781.
[32] Rice MJ, Garstein YN. Phys Rev Lett 1994;73:2504.
[33] da Costa PG, Conwell E. Phys Rev Lett B 1993;48:1993.
[34] Rauscher U, Bässler B, Bradley DDC, Hennecke M. Phys Rev B 1990;42: 9830.
[35] Kersting R, Lemmer U, Mahrt RF, Leo K, Kurz H, Bassler H, et al. Phys Rev Lett 1993;70:3820.
[36] Bassler H, Brandl V, Deussen M, Gobe EO, Kersting R, Kurz H, et al. Pure Appl Chem 1995;67:377.
[37] Hayes GR, Samuel IDW, Phillips RT. Phys Rev Lett B 1995;52:R11569.
[38] Greenham NC, Samuel IDW, Hayes GR, Phillips RT, Kessener YARR, Moratti SC, et al. Chem Phys Lett 1995;241:89.
[39] Blatchford JW, Jessen SW, Lin LB, Lih JJ, Gustafson TL, Epstein AJ, et al. Phys Rev Lett 1996;76:1513.
[40] Halls JJM, Pichler K, Friend RH, Moratti SC, Holmes AB. Appl Phys Lett 1996;68:3120.
[41] Frolov SV, Liess M, Lane PA, Gellermann W, Vardeny ZV, Ozaki M, et al. Phys Rev Lett 1997;78:4285.
[42] Egelhaaf H-J, Bäuerle P, Rauner K, Hoffmann V, Oelkrug D. J Mol Struct 1993;293:249.
[43] Egelhaaf H-J, Bäuerle P, Rauner K, Hoffmann V, Oelkrug D. Synth Met 1994;61:143.
[44] Li R, Bäuerle P, Umbach E. Surf Sci 1995;331–333:100.
[45] Gierschner J, Egelhaaf H-J, Oelkrug D. Synth Met 1997;84:529.
[46] Beljonne D, Cornil J, Brédas JL, Friend RH. Synth Met 1996;76:61.
[47] Chosrovian H, Rentsch S, Grebner D, Dahm DU, Birckner E. Synth Met 1993;60:23.
[48] Janssen RAJ, Moses D, Sariciftci NS. J Chem Phys 1994;101:9519.
[49] Janssen RAJ, Smilowitz L, Sariciftci NS, Moses D. J Chem Phys 1994; 101:1787.
[50] Scaiano JC, Redmond RW, Mehta B, Arnason JT. Photochem Photobiol 1990;52:655.
[51] Xu B, Holdcroft S. J Am Chem Soc 1993;115:8447.
[52] Bennati M, Grupp A, Bäuerle P, Mehring M. Mol Cryst Liq Cryst 1994; 256:751.
[53] Sano Y, Yokohama M, Shirota Y, Mikawa H. Mol Cryst Liq Cryst 1979; 53:291.
[54] IInuma F, Mikawa H, Shirota Y. Mol Cryst Liq Cryst 1981;73:309.
[55] Burkhart RD, Avilles RG. Macromolecules 1979;12:1078.
[56] North AM, Ross DA, Treadaway MF. Eur Polym J 1974;10:411.
[57] Samedova TG, Karpocheva GP, Davydov BE. Eur Polym J 1972;8:599.
[58] Souza JM, dos Anjos PNM, Azevedo WM, Marques AS. J. Luminescence 1999;81:225.